FOUR-BAR LINKAGE SYNTHESIS FOR A COMBINATION OF MOTION AND PATH-POINT GENERATION

Thesis

Submitted to

The School of Engineering of the

UNIVERSITY OF DAYTON

In Partial Fulfillment of the Requirements for

The Degree of

Master of Science in Mechanical Engineering

By

Yuxuan Tong

UNIVERSITY OF DAYTON

Dayton, Ohio

May, 2013

FOUR-BAR LINKAGE SYNTHESIS FOR A COMBINATION OF MOTION AND

PATH-POINT GENERATION

Name: Tong, Yuxuan

APPROVED BY:

Andrew P. Murray, Ph.D.
Advisor Committee Chairman
Professor, Dept. of Mechanical and
Aerospace Engineering

David Myszka, Ph.D.
Committee Member
Associate Professor, Dept. of
Mechanical and Aerospace Engineering

A. Reza Kashani, Ph.D.
Committee Member
Professor, Dept. of Mechanical and
Aerospace Engineering

John Weber, Ph.D.
Associate Dean
School of Engineering

Tony E. Saliba, Ph.D.
Dean, School of Engineering
& Wilke Distinguished Professor

ABSTRACT

FOUR-BAR LINKAGE SYNTHESIS FOR A COMBINATION OF MOTION AND

PATH-POINT GENERATION

Name: Tong, Yuxuan
University of Dayton

Advisor: Dr. Andrew P. Murray

This thesis develops techniques that address the design of planar four-bar linkages for tasks common to pick-and-place devices, used in assembly and manufacturing operations. The analysis approaches relate to two common kinematic synthesis tasks, motion generation and path-point generation. Motion generation is a task that guides a rigid body through prescribed task positions which include position and orientation. Path-point generation is a task that requires guiding a reference point on a rigid body to move along a prescribed trajectory. Pick-and-place tasks often require the exact position and orientation of an object (motion generation) at the end points of the task. Within the range of movement, the motion restrictions are less rigorous with only the position of the object (path generation) being specified to either avoid obstacles or provide direction for a suitable path. Established synthesis theory has been developed for either motion generation or path-point generation tasks. This thesis presents four-bar linkage synthesis methods for tasks that include a combination of motion and path-point generation. This synthesis challenge is addressed via two approaches: Geometric Constraint Programming (GCP) and numerical solutions to synthesis equations. Using

GCP, a step-by-step methodology has been established to find solutions to these synthesis challenges. This technique provides a synthesis process that is intuitive, visual, and avoids the need for the designer to engage in solving complex equations, The drawback to kinematic synthesis using GCP, however, is that only one linkage solution is obtained and sketched by the designer. Using numerical methods, techniques are presented to formulate the kinematic chain constraint equations and solve for the appropriate link lengths and pivot locations. Numerical solutions are generated by the Bertini software package, a program that supports the calculation of large polynomial equations set. Examples of various combinations of motion and path point generation are presented.

ACKNOWLEDGMENTS

I would like to express the deepest appreciation to my committee chair, Professor Andrew P. Murray, who has the attitude and the substance of a genius: he continually and convincingly conveyed a spirit of adventure in regard to research and scholarship, and an excitement in regard to teaching. Without his guidance and persistent help, this dissertation would not have been possible.

I would like to thank my committee members, Professor David Myszka and Professor Reza Kashani, whose work demonstrated to me that a concern for global affairs supported by an engagement in comparative literature and modern technology should always transcend academia and provide a quest for our times.

TABLE OF CONTENTS

LIST OF FIGURES

LIST OF TABLES

CHAPTER I

INTRODUCTION

1.1   Pick and Place Operations

During a typical manufacturing operation, parts are moved from machine to machine and as-
sembled with other parts to form a finished product. These material handling tasks can be completed
manually, or, more commonly, by mechanical devices. Pick-and-place systems, such as those used
in only one possible application, are mechanical devices designed to repetitively perform a specific
sequence of part movements [2]. The application typically requires a part to be picked up from
an initial specific position, oriented into virtually any placing pattern and placed into the expected
position. Design requirements for these systems tend to have rigid end-of-motion constraints. Be-
tween these endpoints, the restriction on the motion tends to be less rigorous and usually consists of
avoiding obstructions.

Pick-and-place systems may be composed of several elements including end effectors, robotic
arms, Human Machine Interfaces (HMI), bracing structures, and basic mechanisms. The device
in Fig. 1.1 [1] is an example of a system with a significant amount of integrated automation with
multiple actuators. The automatic package stamping device, shown in Fig. 1.2 [3], is an example
of a single actuator system with no automation. More sophisticated pick-and-place systems require
high installation accuracy and high maintenance because of the number of components. Such com-
plex mechanisms may prove to be of greater cost to the users than is needed for a pick-and-place

operation. This thesis focuses on the four-bar mechanism as a fundamental machine component that provides significant potential as an element in a fast and inexpensive-to-operate pick-and-place style of machine.
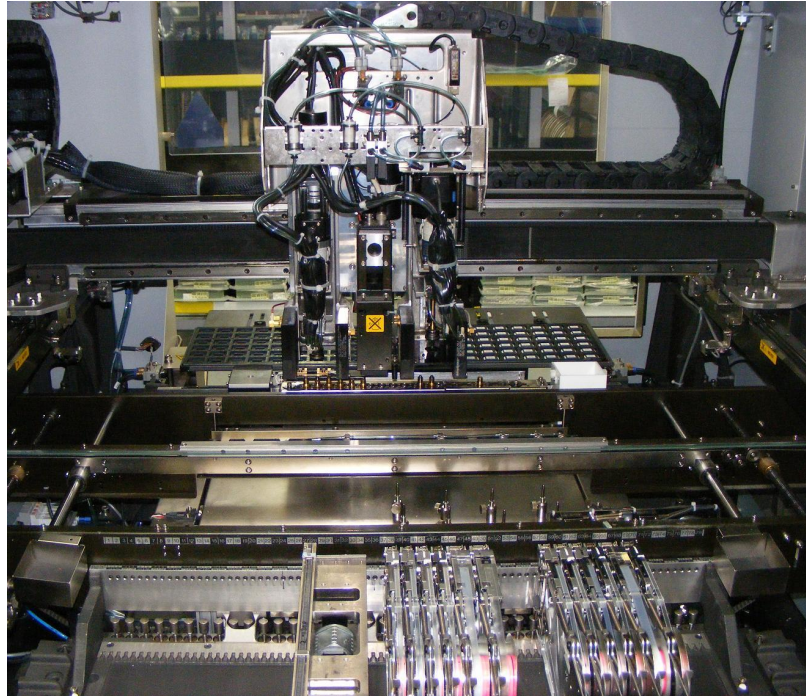
Figure 1.1: Pick-and-place machines may be sophisticated in the amount of robotics integrated into the design

1.2 Dimensional Synthesis of Linkages

Dimensional synthesis is a process to determine the dimensions for a preconceived type of linkage to perform a desired task [3]. Dimensional synthesis is often divided into three categories of tasks: function generation, path-point generation and motion generation. The goal of function generation is to coordinate the motion of links within a mechanism and is not studied here. The latter two, path-point and motion generation, directly apply to pick-and-place operations. Path-point
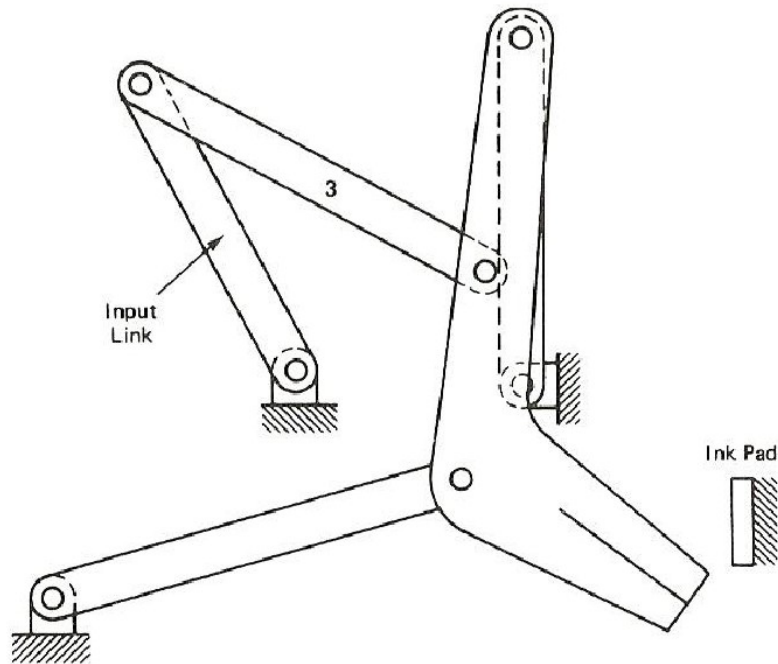
Figure 1.2: A fast and inexpensive-to-operate pick-and-place style of machine

generation requires guiding a reference point on a rigid body to meet points along a prescribed trajectory. The required positions of the reference point are termed precision points. Motion generation, also called rigid-body guidance, is a task that guides a rigid body through prescribed positions and orientations. The position and orientation of the guided rigid-body at the designated location is called a task position.

The theory of motion generation is a problem that has received considerate attention by linkage designers [3, 4]. Well established methods have been developed to generate chains composed of two links and two revolute (R) joints, termed RR dyads. To formulate constraint equations, the orientation of the distal link and the position of a reference point on that link serve as a task position. The location of the fixed R joint, the moving R joint, and the length of the link between them are the variables to be determined. Solving for two such RR dyads allows them to be jointed into a single

3

four-bar mechanism. The maximum number of task positions is 5, there are at most 4 RR dyads that reach the 5 task positions [5]. For 4 task positions, a curve of solutions called a center-point curve results. This curve was originally formulated by Burmester [6]. The curve is the locus of fixed pivot locations for an RR dyad that will guide the distal link through the 4 task positions. The synthesis of four-bar mechanism to achieve up through 5 task positions is covered in many texts in the theory of machines field including, for example, [3, 4].

Whereas motion generation may be solved by coupling RR dyads, the process for path-point generation is performed for the entire four-bar linkage. The reason for working with the entire mechanism is that finding individual RR dyads to meet the precision points is trivial. Two of them, however, cannot be coupled as the amount of rotation between precision points of the distal link is not the same for the two RR dyads. Freudenstein and Sandor [7] produced closed form solutions for up to 4 precision points. Suh and Radcliffe [8] introduced a set of simultaneous nonlinear equations for five precision points, which they solved numerically. Morgan and Wampler [9] utilized continuation methods, like those described in significant detail in Ch. 4 of this thesis, to solve for the theoretical maximum of 9 precision points. Further, Wampler [10] solved a problem with randomly generated precision points and generated 1442 sets of Robert's cognate triples ($1442 \times 3 = 4326$ solutions).

Approximate-position synthesis [11] focuses on generating mechanisms to traverse the task positions or precision points within an acceptable error range. The process acknowledges that no exact solution is likely to be found and so a metric needs to be introduced to decide if the device achieves acceptable accuracy. A set of thorough references on appropriate synthesis can be found in Diab and Smaili [12]. For a recent approach, see Plecnik and McCarthy's work on five position synthesis of a slider-crank function generator [13]. Mirth [14] presented the example of tolerance

zones for linkage synthesis, called quasi-positions, and his work was continued by Holte [15]. The four approximately specified positions was analyzed by Mlinar and Erdman [16].

Traditional techniques for kinematic synthesis of planar mechanism tend to focus on three approaches: trial and error, graphical techniques, and analytical techniques. Using trial and error, motion of a mechanism can be generated. Adjusting the parameters of the mechanism, either graphically or numerically, the mechanism is inspected to see if it satisfies the design requirements. Using this approach, it can be difficult to generate accurate solutions. Also, due to the highly nonlinear behavior of most mechanisms, the design work may become tedious. Graphical techniques generate solutions quickly and accurately when the techniques exist. Typically, these techniques are in place only for the most straightforward of kinematic synthesis challenges. The final methodology, analytical techniques, can produce highly accurate solutions. The problem with this technique is the extensive calculations or numerical methods required to solve the system of equations. A balanced understanding of the approaches tends to yield the most insight.

Linkage synthesis can produce unacceptable solutions that suffer from circuit defects, branch defects, or order defects [19, 20]. Linkage synthesis solutions, whether through numerical or GCP techniques must be checked for defects, a process termed solution rectification. Balli and Chand completed a comprehensive overview of linkage defects and solution rectification [21].

1.3 Geometric Constraint Programming

Geometric Constraint Programming (GCP) was first introduced by Kinzel [17]. This paper addressed the original GCP techniques based on the four-bar mechanism synthesis of motion generation (finitely separated position generation), path-point generation, and function generation. GCP is based on the set of tools available in most CAD packages that allow for the specification of relationships between geometric entities (line segments and circles) while allowing the lengths and

positions of those entities to vary. The benefit of GCP is that the synthesis process is intuitive, visual, and avoids the need for the designer to engage in solving complex equations. Additional research has been extended GCP to address the constraint force design method [22], the geometric constraint engine for the collection of entities under geometric constraints [23], and the function generation using geometric constraint programming [24].

GCP is a technique that has the advantages of both the graphical and analytical techniques. The sketching of a mechanism and the constraints on its motion are created in the CAD tools and the user avoids the analytical aspects of solving the problem. CAD packages provide the user with basic graphical entities (line segments and circles, etc.) and allows for their creation and constraint definition. Common CAD packages offer the user a set of constraint tools for the specification of relationships between geometric entities which allow the lengths and positions of those entities to be variables. SolidEdge [18] is used in this work and has the appropriate suite of tools available as part of its freeware version, noting that AutoCAD, SolidWorks and Inventor are other readily available options.

The necessary graphical constraints for kinematic synthesis include: strong connect, weak connect, dimension lock, position lock, equality, parallelism, perpendicularity, and tangency. A revolute joint is restricted by a "strong connect". That is, when the endpoints of the lines are forced to be coincident, they behave as if connected by a revolute joint. A simple slider system is restricted by a "weak connect" between slider and trajectory, in order to free the slider sliding along the track in the tangential direction. A "position lock" is used for locating the task position in the fixed frame.

The constraints toolbar in SolidEdge is shown in Fig. 1.3. The constraints described above are located on the constraint toolbar as strong and weak connect in "Tool 1", parallelism in "Tool 2", lock in "Tool 3" and equality in "Tool 4". In short, the designer sketches the task positions and a potential solution (using the CAD package's drafting tools) and then applies the geometric

constraints that make the potential solution conform to being an actual solution. Thus, the constraint

solver in the CAD package determines a local solution to the imposed constraints.
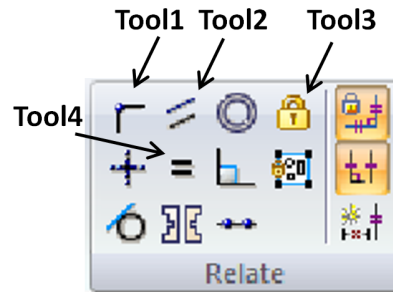
Figure 1.3: The "constraint toolbar" in SolidEdge.

Utilizing GCP for combined motion generation with path-point generation design problems is

highly consistent. Since the variables in GCP are lines representing the links, the difference between

motion and path-point generation synthesis is merely the number of constraints applied. Thus,

for synthesis challenges that involve both motion and path-point generation, GCP can be readily

applied. The drawback to kinematic synthesis using GCP is that only one solution is obtained; the

one closest to the potential solution sketched by the designer.

1.4 Polynomial Homotopy

Solving the constraint equations for motion or path-point generation generates all possible so-

lutions but can be a challenging task. Recent developments in the mathematical theory of polyno-

mials have created new methods of solution called continuation (or homotopy) methods. Wampler

[25, 27, 26] presented techniques for using isotropic coordinates to generate polynomial equations

that describe the position of a general single-DOF linkage that, so far as can be checked, gives

the lowest degree polynomial equation relating the input to the output. Solution of the complex,

polynomial systems can be readily accomplished by using numerical polynomial continuation [28]. Polynomial continuation is so useful here because it generates all solutions to a system of algebraic polynomial equations.

Software for polynomial continuation is available in the Bertini software package [29]. Bertini produces all isolated solutions of a system of polynomials with complex coefficients. Moreover, due to its use of multiple precision, the isolated solutions can be computed with up to several hundred digits of accuracy.

The polynomial equation systems can be solved by Bertini if the coefficients are complex numbers and the power of the variables are positive. As a simple example, the equation $a\mathbf{x}^2 + b\mathbf{x} + c = 0$ can be solved when a, b and c are complex numbers. On the contrary, the equation $a\ sin^2(x) + b\ cos(x) + c = 0$ is not solvable using Bertini.

1.5   Organization

The remainder of the thesis is organized as followed. The design equations for a single RR dyad, and a four-bar linkage are presented in Ch. 2. GCP synthesis methods for path-point, motion generation and a combination of tasks is given in Ch. 3. Chapter 4 discusses numerical synthesis methods for a combination of specified tasks, and examples. Chapter 5 presents the conclusion and future work.

CHAPTER II

KINEMATIC BACKGROUND

2.1 Modeling with Isotropic Coordinates

Vectors representing a single RR dyad consisting of a proximal link and distal link are shown in Fig. 2.1. This is identified as dyad 1 to distinguish it from a second dyad included later. The location of the fixed pivot relative to a fixed frame F is $\mathbf{G}_1$ and the length of the proximal link is L_1. The jth task position is described by a coordinate system M_j and is defined by a location vector $\mathbf{d}_j$ and an orientation angle θ_j, both relative to a fixed frame F. Correspondingly, the position of the the proximal link at the jth task position is represented by $\mathbf{L}_{1j}$

In kinematic formulations, it is common to use vectors in the complex plane [3]. That is, the displacement vector is specified relative to F as $\mathbf{d}_j = d_{jx} + i\, d_{jy}$, having a complex conjugate $\overline{\mathbf{d}}_j = d_{jx} - i\, d_{jy}$, where $i = \sqrt{-1}$. Similarly, the location of the fixed pivot (also known as the center-point) relative to F is $\mathbf{G}_1 = G_{1x} + i\, G_{1y}$, having a complex conjugate $\overline{\mathbf{G}}_1 = G_{1x} - i\, G_{1y}$. The location of the moving pivot (also known as the circle-point) relative to M_j is $\mathbf{z}_1 = z_{1x} + i\, z_{1y}$, having a complex conjugate $\overline{\mathbf{z}}_1 = z_{1x} - i\, z_{1y}$.

To describe the orientation angle, a unit vector defined by θ_j is represented in polar form as,

$$\mathbf{T}_j = e^{i\theta_j}. \tag{2.1}$$
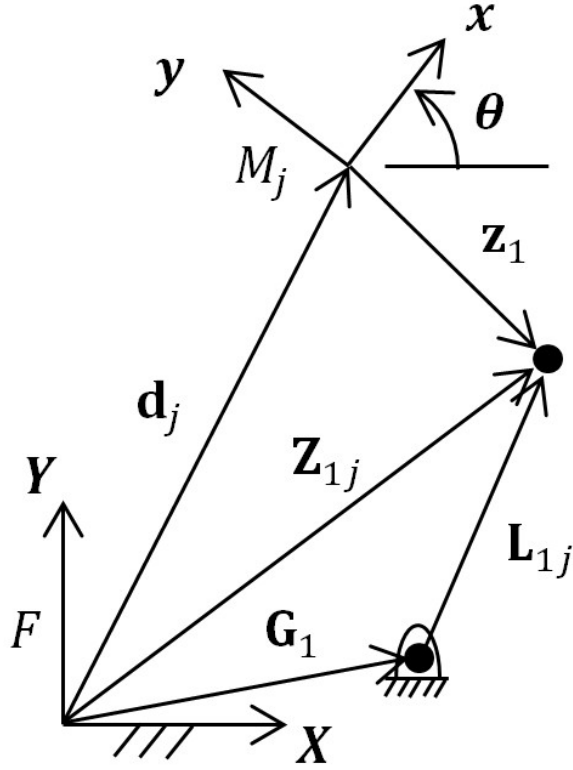
Figure 2.1: Vectors representing a single RR dyad.

Applying the Euler identity, the components of the unit vector are

$$\mathbf{T}_j = \cos\theta_j + i\sin\theta_j. \tag{2.2}$$

The complex conjugate of $\mathbf{T}_j$ is

$$\overline{\mathbf{T}}_j = e^{-i\theta_j} = \cos\theta_j - i\sin\theta_j, \tag{2.3}$$

and

$$\mathbf{T}_j\overline{\mathbf{T}}_j = e^{i\theta_j}e^{-i\theta_j} = 1. \tag{2.4}$$

Mechanism links that are represented by exponential variables and their conjugates are isotropic coordinates. A more complex discussion of isotropic coordinates and their properties can be found in Wampler [26].

10

Using the isotropic formulation, the coordinates of the circle-point in F are

$$\mathbf{Z}_{1j} = \mathbf{T}_j \mathbf{z}_1 + \mathbf{d}_j. \tag{2.5}$$

Alternatively, the location of the moving pivot relative to the fixed frame as constrained by the crank is

$$\mathbf{Z}_{1j} = \mathbf{G}_1 + \mathbf{L}_{1j} \tag{2.6}$$

Combining Eqs. 2.5 and 2.6,

$$\mathbf{L}_{1j} = \mathbf{T}_j \mathbf{z}_1 + \mathbf{d}_j - \mathbf{G}_1. \tag{2.7}$$

The complex conjugate of Eq. 2.7 is

$$\overline{\mathbf{L}}_{1j} = \overline{\mathbf{T}}_j \overline{\mathbf{z}}_1 + \overline{\mathbf{d}}_j - \overline{\mathbf{G}}_1, \tag{2.8}$$

noting that $\mathbf{L}_{1j} \overline{\mathbf{L}}_{1j} = (L_1)^2$.

Dimensional synthesis of an RR dyad amounts to determining appropriate values of $\mathbf{G}_1$ and $\mathbf{z}_1$. The fundamental synthesis equation must guarantee a constant proximal link length, which is ensured by

$$\mathbf{L}_{1j} \cdot \overline{\mathbf{L}}_{1j} - \mathbf{L}_{11} \cdot \overline{\mathbf{L}}_{11} = 0. \tag{2.9}$$

where $j = 2, \ldots, n$ for n task specifications. Equation 2.9 relates the task specifications to the synthesis values ($\mathbf{G}_1$ and $\mathbf{z}_1$). For motion generation, θ_j (or $\mathbf{T}_j$) and $\mathbf{d}_j$ are the given task specifications, whereas only $\mathbf{d}_j$ is given for the path-point generation and the corresponding $\mathbf{T}_j$ is regarded as unknown.

A complete four-bar linkage consists of two RR dyads and the vector representation is shown in Fig. 2.2. Identical equations can be formulated for the second RR dyad, which forms a second synthesis equation,

$$\mathbf{L}_{2j} \cdot \overline{\mathbf{L}}_{2j} - \mathbf{L}_{21} \cdot \overline{\mathbf{L}}_{21} = 0. \tag{2.10}$$
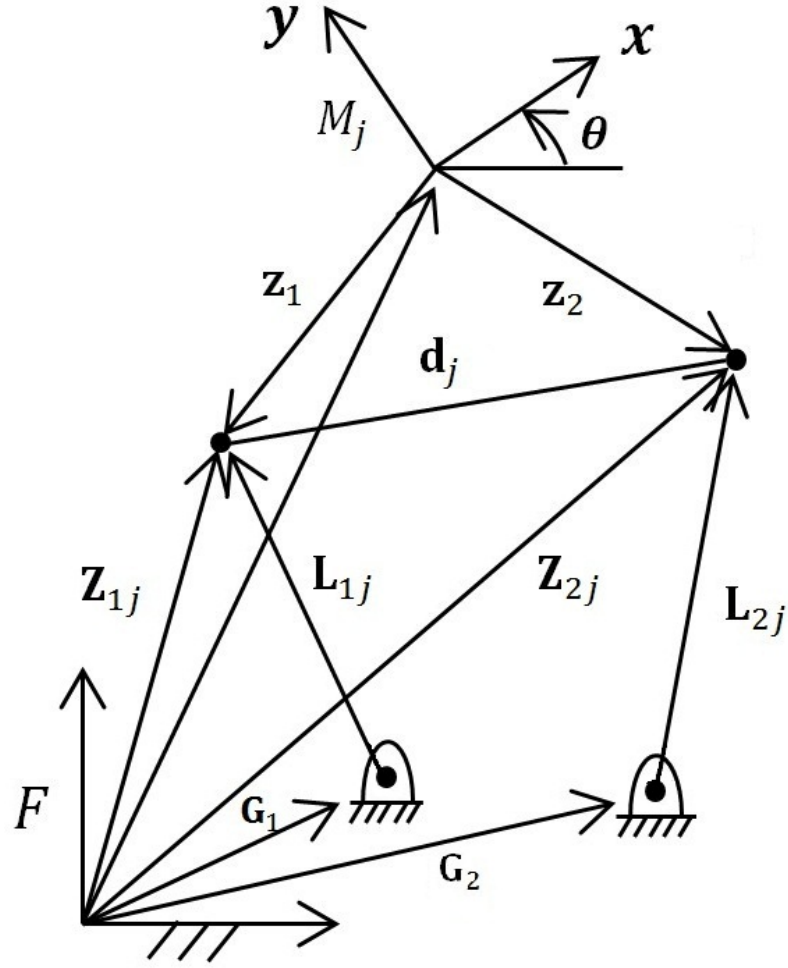
Figure 2.2: Vectors representing two RR dyads, forming a four-bar linkage.

2.2 Parallelism in Isotropic Coordinates

In Ch. 4, the fact that two parts of isotropic coordinates are parallel is useful. Given that $\mathbf{A}$ and $\mathbf{B}$ are nonzero complex numbers, then

$$\mathbf{A}\overline{\mathbf{B}} - \overline{\mathbf{A}}\mathbf{B} = 0 \qquad (2.11)$$

implies that $\mathbf{A}$ and $\mathbf{B}$ are parallel. This proof is taken from [30]. Multiplying Eq. 2.11 by $\mathbf{AB}$,

$$\mathbf{A}^2\,\overline{\mathbf{B}}\mathbf{B} - \overline{\mathbf{A}}\mathbf{A}\mathbf{B}^2 = 0.$$

As shown in Eq. 2.4, $\overline{\mathbf{A}}\mathbf{A} = a^2$ and $\overline{\mathbf{B}}\mathbf{B} = b^2$, where a and b are the lengths of $\mathbf{A}$ and $\mathbf{B}$, respectively. So the expression factors as

$$(b\mathbf{A} + a\mathbf{B})(b\mathbf{A} - a\mathbf{B}) = 0.$$

which requires either $(b\mathbf{A} + a\mathbf{B}) = 0$ or $(b\mathbf{A} - a\mathbf{B}) = 0$. If $(b\mathbf{A} + a\mathbf{B}) = 0$ then $\mathbf{A}$ and $\mathbf{B}$ are in opposite directions. If $(b\mathbf{A} - a\mathbf{B}) = 0$, then $\mathbf{A}$ and $\mathbf{B}$ are in the same direction. In either case, $\mathbf{A}$ and $\mathbf{B}$ are parallel.

2.3   Formulation of the Design Equations

For synthesis problems that generate a finite set of solutions, the equations for both dyads are formulated to produce a system to be solved. For the 5 task positions problem, discussed earlier, a system is constructed from Eqs. 2.9 and 2.10 with $j = 2, \ldots, 5$. The known quantities specified by the 5 task positions are $\mathbf{d}_j$, $\mathbf{T}_j$ for $j = 1, \ldots 5$. This produces a system of 8 equations in the 8 complex variables of $\mathbf{G}_1$, $\mathbf{G}_2$, $\mathbf{z}_1$, $\mathbf{z}_2$, $\overline{\mathbf{G}}_1$, $\overline{\mathbf{G}}_2$, $\overline{\mathbf{z}}_1$, $\overline{\mathbf{z}}_2$.

Solving this system is not the ideal methodology for motion generation. The ideal solution methodology with more compact modeling equations for 5 task position motion generation, are introduced in the previous research mentioned in Sec. 1.2. These less than ideal equations are introduced here due to the consistency in the formulation needed for the more complex problems to come.

Also mentioned earlier was the 9 precision point problem, which also produces a discrete number of solutions. A system is constructed from the identity Eq. 2.4, and Eqs. 2.9 and 2.10 with $j = 2, \ldots, 9$. The known quantities specified by the 9 precision points are $\mathbf{d}_j$, for $j = 1, \ldots 9$ and $\mathbf{T}_1$ to designate a reference. Thus, this system is composed of 24 equations in the 24 complex variables $\mathbf{G}_1$, $\mathbf{G}_2$, $\mathbf{z}_1$, $\mathbf{z}_2$, $\overline{\mathbf{G}}_1$, $\overline{\mathbf{G}}_2$, $\overline{\mathbf{z}}_1$, $\overline{\mathbf{z}}_2$, $\mathbf{T}_j$, $\overline{\mathbf{T}}_j$, $j = 2, \ldots, 9$.

A similar system of equations can be generated for different combinations of path-point and motion generation specification that produces finite solutions. For an application that requires 4 task positions and 2 precision points, a system is constructed from Eqs. 2.9 and 2.10 with $j = 2, \ldots, 6$ and Eq. 2.4 with $j = 5, 6$. The known quantities specified by the 4 task positions are $\mathbf{d}_j$, $\mathbf{T}_j$ for $j = 1, \ldots 4$. The known quantities specified by the 2 precision points are $\mathbf{d}_j$ for $j = 5, 6$. This system consists of 12 equations in the 12 complex variables of $\mathbf{G}_1$, $\mathbf{G}_2$, $\mathbf{z}_1$, $\mathbf{z}_2$, $\mathbf{T}_5$, $\mathbf{T}_6$ $\overline{\mathbf{G}}_1$, $\overline{\mathbf{G}}_2$, $\overline{\mathbf{z}}_1$, $\overline{\mathbf{z}}_2$, $\overline{\mathbf{T}}_5$, $\overline{\mathbf{T}}_6$.

As another example, the combination of 2 task positions and 6 precision points necessitates Eqs. 2.9 and 2.10 with $j = 2, \ldots, 8$, and Eq. 2.4 with $j = 3, \ldots, 8$. The known quantities specified by the 2 task positions are $\mathbf{d}_j$, $\mathbf{T}_j$ for $j = 1, 2$. The known quantities specified by the 6 precision points are $\mathbf{d}_j$ for $j = 3, \ldots, 8$. This generates 20 equations in the 20 complex variables of $\mathbf{G}_1$, $\mathbf{G}_2$, $\mathbf{z}_1$, $\mathbf{z}_2$, $\overline{\mathbf{G}}_1$, $\overline{\mathbf{G}}_2$, $\overline{\mathbf{z}}_1$, $\overline{\mathbf{z}}_2$, $\mathbf{T}_j$, $\overline{\mathbf{T}}_j$, $j = 3, \ldots, 8$.

When working in isotropic coordinates the term "real solution" takes on an unusual meaning. Since Bertini generates all possible solutions on the domain of complex numbers to a set of equations, the solution set must be post-processed to verify that it is a "real solution". From the perspective of the software, $\mathbf{G_1}$ and $\overline{\mathbf{G}}_1$ are entirely separate variables. Thus, a viable solution has the property that $\mathbf{G}_1$ and $\overline{\mathbf{G}}_1$ are complex conjugates, and solutions exist to the system of equations for which that is not the case. Likewise, $\mathbf{G}_2$ and $\overline{\mathbf{G}}_2$, $\mathbf{z}_1$ and $\overline{\mathbf{z}}_1$, $\mathbf{z}_2$ and $\overline{\mathbf{z}}_2$ and $\mathbf{T}_j$ and $\overline{\mathbf{T}}_j$ must be complex conjugates. Moreover, the variables $\mathbf{T}_j$ or $\overline{\mathbf{T}}_j$ being "real" is taken to mean that the corresponding angle θ_j is real. This implies that $|\mathbf{T}_j| = |\overline{\mathbf{T}}_j| = 1$, which must be verified after finding the solution.

Table 2.1 presents all the combination of precision points and task positions that produce a finite number of solutions. Note that because an angle specification is required as a reference for the 9 precision points case, combinations of 1-position 8-points and 0-position 9-points are the same.

14

Table 2.1: Combinations of task positions and precision points that have a finite number of four-bar linkage solutions

No. of Task Positions:	5	4	3	2	1	0
No. of Precision Points:	0	2	4	6	8	9
No. of Eqs. and Variables	8	12	16	20	24	24

CHAPTER III

GCP APPROACHES FOR COMBINED PATH-POINT AND MOTION GENERATION

A four-bar linkage as represented by lines typical of the sketching tool in most CAD packages is shown in Fig. 3.1. When the linkage moves from one task position to another, the two moving pivots (circle points) must lie on circles and the fixed pivots are the center points of those circles. Obtaining a linkage solution that performs the designated task involves finding the size of the circles and their center points.

3.1   Path-Point Generation

Figure 3.2 shows a typical GCP construction for path-point generation. In this case, a four-bar linkage is desired that guides a point on the coupler through 2 precision points, A_1 and A_2. Note the two triangles $A_1B_1C_1$ and $A_2B_2C_2$ represents the coupler of the four-bar linkage in two poses. A "strong connect" constraint is used to ensure that the endpoints of the lines remain coincident to form the triangles. The coupler reference point, A_1 and A_2, is anchored as speficied by the precision points. The "position lock" constraint is used to anchor the points.

All the triangles that represent the coupler must be congruent with each other. That is, $\|A_1B_1\|$ =$\|A_2B_2\|$, $\|B_1C_1\|$ =$\|B_2C_2\|$ and $\|A_1C_1\|$ =$\|A_2C_2\|$, where $\|AB\|$ is the length of the line that
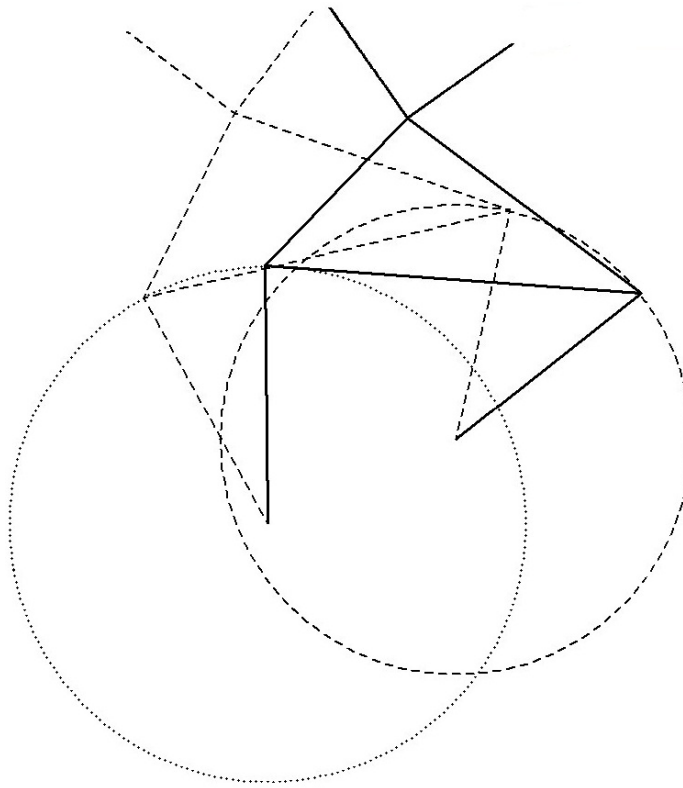
Figure 3.1: The circle and center points that define a four-bar linkage capable of guiding a body between two positions

joins points A and B. Correspondingly, an "equality" constraint is specified between the appropriate legs of the triangles.

Also, note that vertex B lies on the light dashed circle, and vertex C lies on the heavy dashed circle. Thus, a "weak connect" between the vertices of the triangles and the circles is used to ensure that the vertices lie on the circle, but allow the vertices to slide along it.

The unconstrained geometry includes the center and size of each circle and the length of each line in the triangle. Numerically enforcing the constraints while the geometry is modified is not a trivial task, but the constraint solvers found in CAD packages are well suited to this activity. Therefore, designers can vary the circles and triangles while maintaining the constraints, until a
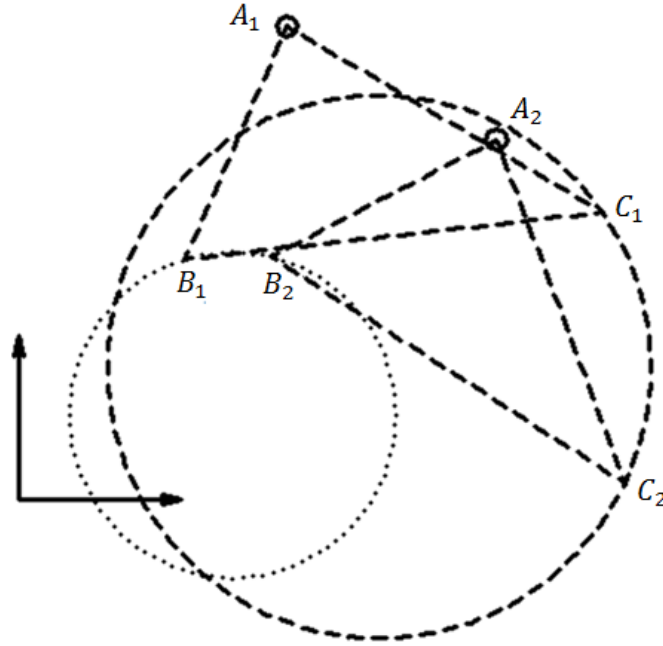
Figure 3.2: GCP is used to solve path-point synthesis problem with 2 precision points.

desirable linkage is obtained. As more precision points are added to the sketch, there is less freedom to resize the sketch. With 9 precision points, the designer is theoretically able to "snap" between a discrete number of linkage solutions. In practice, once a solution is found, it can be difficult to "snap" to another linkage solution.

3.2 Motion Generation

Figure 3.3 shows a typical GCP construction for motion generation. In this case, a mechanism is desired that guides a body through 2 task positions indicated by the solid reference frames. As before, triangles $A_1 B_1 C_1$ and $A_2 B_2 C_2$ represents the coupler of the four-bar linkage in two poses. The reference point, A_1 and A_2, is anchored as specified by the task position. The triangles, and two circles are constructed and constrained in an identical manner to the path-point construction.

18
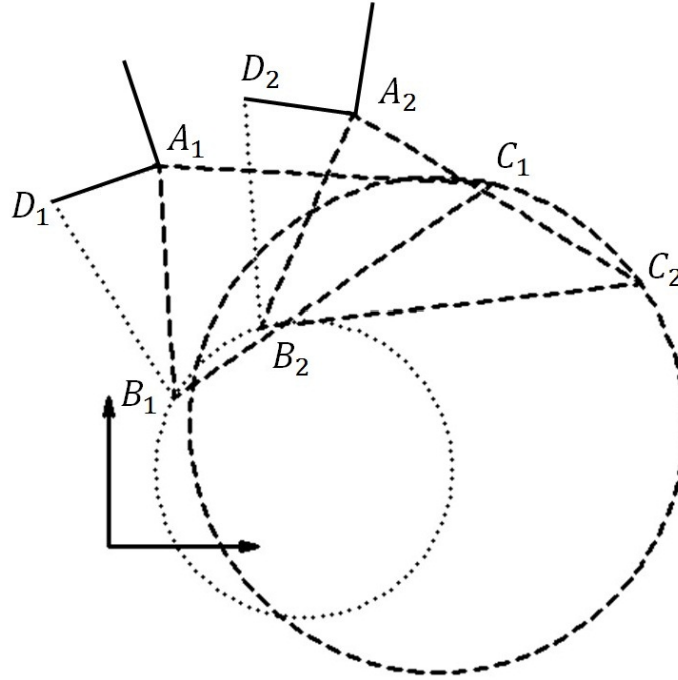
Figure 3.3: GCP is used to solve a motion generation problem with 2 task positions.

Additional triangles $A_1B_1D_1$ and $A_2B_2D_2$ are constructed such that the vertices D_1 and D_2 connect to a point on the reference frame. These additional triangles established the orientation of the coupler at the task position. These additional triangles must also be congruent, adding two more constraints $\|A_1D_1\| = \|A_2D_2\|$ and $\|B_1D_1\| = \|B_2D_2\|$. As before, an "equality" constraint is used to specify these conditions.

The unconstrained geometry remains the center and size of each circle and the length of each line in both triangles. As before, designers can vary the circles and triangles, but less freedom is observed. As more task positions are added to the sketch, there is less freedom to resize the sketch. With 5 task positions, the designer is theoretically able to "snap" between a discrete number of linkage solutions.

3.3 Combining Path and Motion Generation

Pick-and-place applications involve a combination of precision points and task positions. Fig. 3.4 shows a combined task problem with 1 task position and 1 precision point. It is clearly seen that a suitable linkage is obtained by a combining the two methods discussed above.
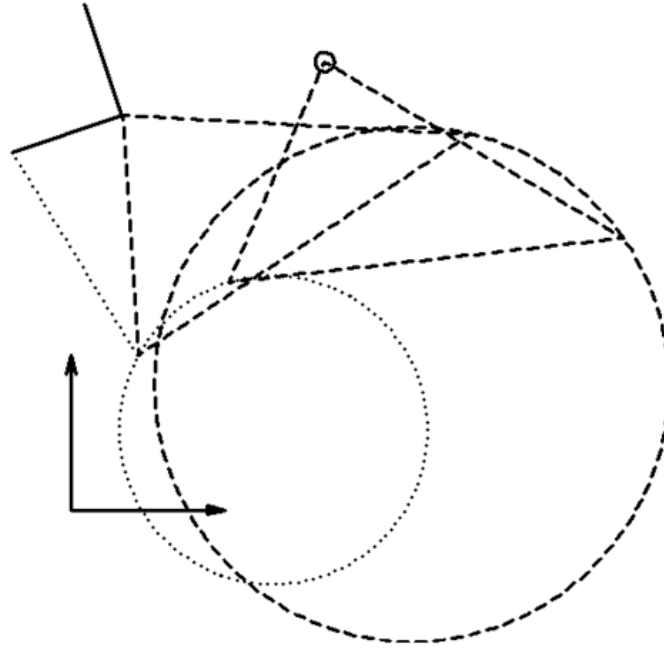
Figure 3.4: Using GCP to solve a combined synthesis problem with 1 task position and 1 precision point

3.4 GCP Examples

3.4.1 4 Task Position and 2 Precision Point Example

As Table 2.1 specifies, 4 task positions and 2 precision points defines a finite number of four-bar mechanisms. Table 3.1 lists the 4 task positions and 2 precision points for an example design problem. After constructing all triangles and circles as described in Secs. 3.1-3.3, a solution is

readily generated and shown, with the design problem, in Fig. 3.5. For sake of clarity, not all triangles are shown in the figure. The trajectory of a point on the coupler is also shown as passing through the origins of the 4 task positions and the 2 precision points. Note that, as this problem has a finite number of solutions, the design in Fig. 3.5 cannot be continuously varied to another potential solution. When constraints are related and features of the mechanism altered, the solver usually converges back to the same solution. This is a potential issue for considering alternate designs to the same problem.

Table 3.1: GCP methodology for the combined task consisting of 4 task positions and 2 precision points

j	d_{j_x}	d_{j_y}	θ_j(deg)
1	11.39	27.51	110.84
2	13.95	29.06	101.73
3	18.86	30.01	–
4	19.85	30.01	–
5	23.99	28.87	64.30
6	28.00	24.80	35.17

3.4.2 3 Task Position and 3 Precision Point Examples

Table 3.2 lists the 3 task positions and 3 precision points for an example design problem. After constructing all triangles and circles as described in Secs. 3.1-3.3, a solution is readily generated and shown, with the design problem, in Fig. 3.6. For sake of clarity, not all triangles are shown in the figure. The trajectory of a point on the coupler is also shown as passing through the origins of the 3 task positions and the 2 precision points. Note that, as this problem has an infinite number of solutions, the design in Fig. 3.6 is readily varied to another potential solution, as shown in Fig 3.7.

21
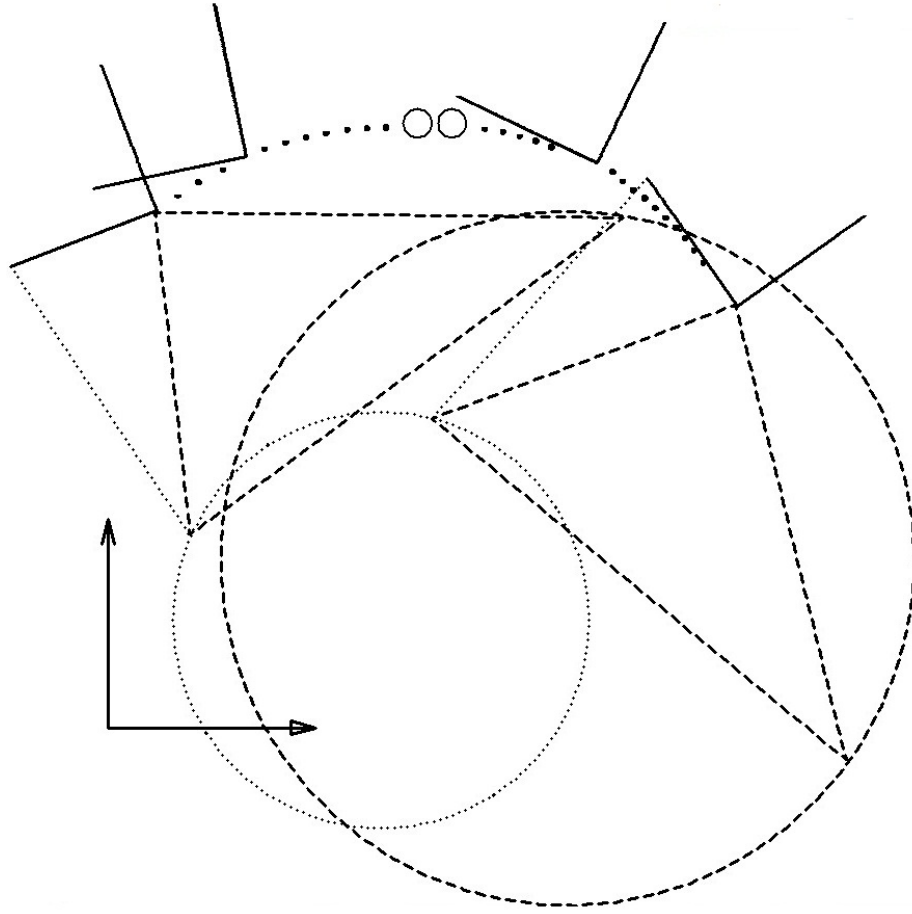
Figure 3.5: The solution generated by GCP for the task in Table 3.1.

3.4.3   Other Examples

In this research, several examples were generated using the GCP technique. Additional trials included the following combinations: 5 task positions and 0 precision point, 0 task position and 9 precision points, 3 task positions and 2 precision points. The examples are not shown here, but GCP techniques readily generated at one solution to these challenges.

Table 3.2: GCP methodology for the combined task consisting of 3 task positions and 3 precision points

j	d_{j_x}	d_{j_y}	θ_j(deg)
1	11.39	27.51	110.84
2	13.95	29.06	–
3	18.86	30.01	–
4	19.85	30.01	–
5	23.99	28.87	64.30
6	28.00	24.80	35.17
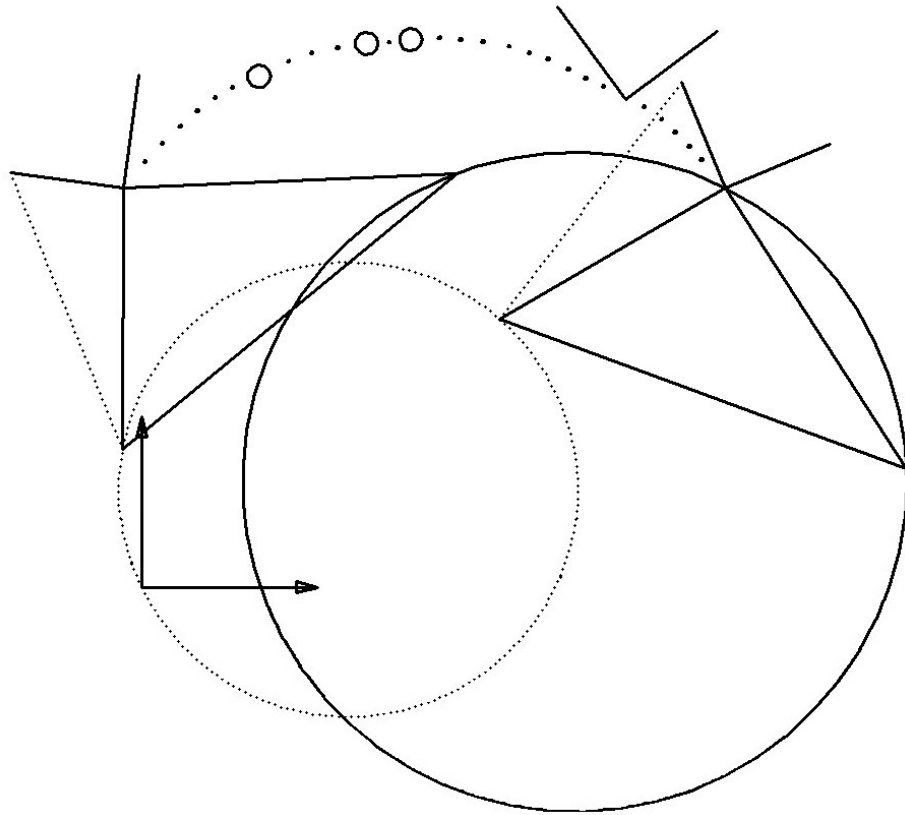
Figure 3.6: The solution generated by GCP for the task in Table 3.2.
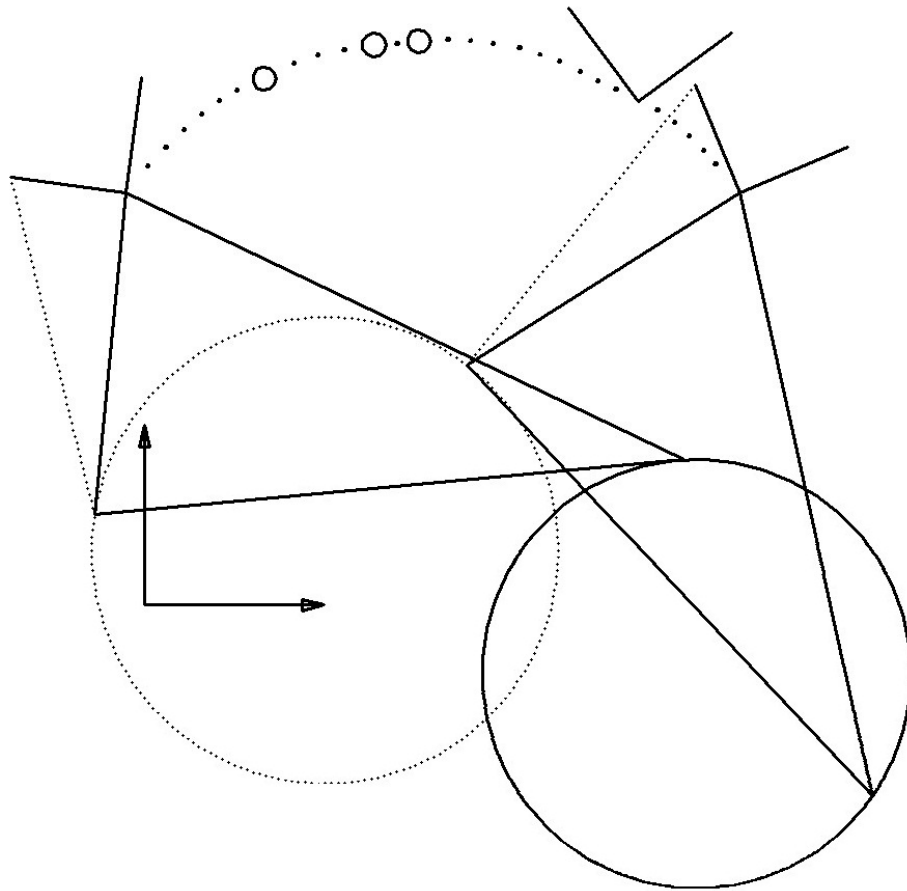
Figure 3.7: The second solution generated by GCP for the task in Table 3.2.

CHAPTER IV

NUMERICAL EXAMPLES OF COMBINED PATH-POINT AND MOTION

GENERATION

GCP is a practical tool with high precision and efficiency for the design of a pick-and-place systems. GCP readily generates a single solutions for a four-bar mechanism that satisfies the task specifications. However, GCP cannot solve for all possible solutions. Therefore, numerical methods are used to obtain all feasible solutions or present a design with an array of solutions to a given problem.

4.1   Combinations having Finite Solutions

The numerical solution of a large set of polynomial equations is effectively accomplished through homotopy methods. Methods for doing so are discussed in [28] and are available in the Bertini software package. The combinations of path point and motion generation problems that have finite solutions was presented in Table 2.1. Generating the set of synthesis conditions from Eq. 2.4, Eqs. 2.9 and 2.10 was discussed in Ch. 2. Methods for doing so are available in the Bertini software package.

4.1.1   4 Task Position and 2 Precision Point Example

A four-bar mechanism is desired to guide a rigid body through the 4 task positions and 2 precision points given in Table 4.1. The equation, as presented in Ch. 2 applied to this problem are,

$$\mathbf{L}_{1j} \cdot \overline{\mathbf{L}}_{1j} - \mathbf{L}_{11} \cdot \overline{\mathbf{L}}_{11} = 0 \qquad \mathbf{L}_{2j} \cdot \overline{\mathbf{L}}_{2j} - \mathbf{L}_{21} \cdot \overline{\mathbf{L}}_{21} = 0, \qquad j = 2, \dots, 6. \tag{4.1}$$

Since the orientation for precision-points 3 and 4 are variables,

$$\mathbf{T}_j \overline{\mathbf{T}}_j = 1, \qquad j = 3, 4. \tag{4.2}$$

This polynomial system of 12 equations in the 12 complex variables maybe listed in two groups as $\{\mathbf{G}_1, \mathbf{G}_2, \mathbf{z}_1, \mathbf{z}_2, \mathbf{T}_3, \mathbf{T}_4\}$ and $\{\overline{\mathbf{G}}_1, \overline{\mathbf{G}}_2, \overline{\mathbf{z}}_1, \overline{\mathbf{z}}_2, \overline{\mathbf{T}}_5, \overline{\mathbf{T}}_6\}$.

Table 4.1: Combined task consisting of 4 task positions and 2 precision points

j	d_{j_x}	d_{j_y}	θ_j
1	15.95	29.38	102.07
2	19.84	32.66	91.72
3	26.90	34.41	–
4	32.66	32.93	–
5	37.40	29.06	53.52
6	40.00	26.59	30.45

Using polynomial continuation as implemented in the Bertini software, 2520 paths were tracked resulting in 156 solutions. As introduced in Sec. 2.3, the solution set must be post-processed to verify that it is a "real solution". Thus, $\mathbf{G}_1$ and $\overline{\mathbf{G}}_1$, $\mathbf{G}_2$ and $\overline{\mathbf{G}}_2$, $\mathbf{z}_1$ and $\overline{\mathbf{z}}_1$, $\mathbf{z}_2$ and $\overline{\mathbf{z}}_2$ and $\mathbf{T}_j$ and $\overline{\mathbf{T}}_j$ must be complex conjugates. For the variables $\mathbf{T}_j$ and $\overline{\mathbf{T}}_j$ to be "real", $|\mathbf{T}_j| = |\overline{\mathbf{T}}_j| = 1$. After post-processing, 22 real solutions as generated by Bertini which corresponds to 11 actual mechanisms were found. The solutions for G_{1x} and G_{1y} are shown as isolated points in Fig. 4.1 (3

of the solutions are not shown as they are outside the figure). The center-point curve for the 4 task positions is also shown. Clearly, the G_1 and G_2 solutions to the 4 task positions 2 precision points problem must lie on that curve. The choice of any G_1 is associated with one other point on the curve, G_2. Figure 4.2 gives one solution assembled into a linkage that can successfully accomplish the 4 task position and 2 precision point task. All solutions to this problem are listed in Table 4.2. Note that a pairing of G_1 and G_2 may be reversed to generate a second solution in Bertini, which explains why the number of solutions is twice the number of actual mechanisms.
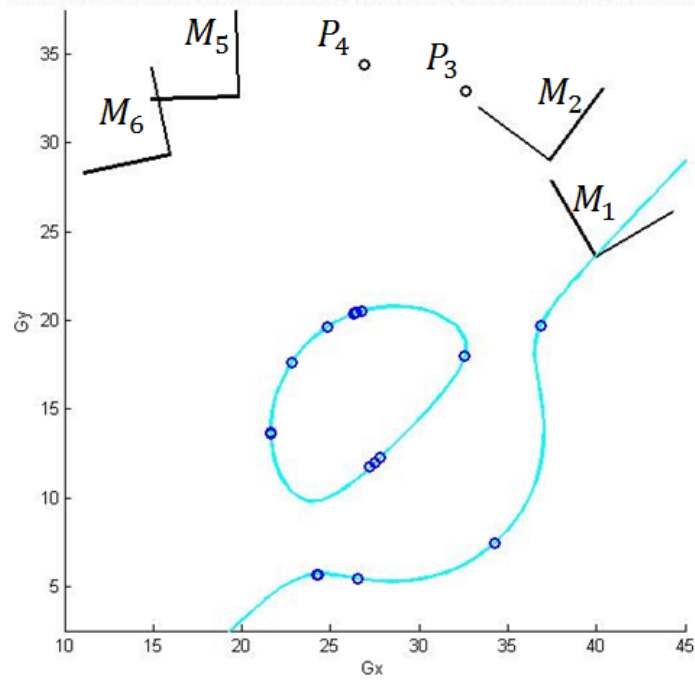

Figure 4.1: G_{1x} and G_{1y} solutions that satisfy the task in Table 4.1.

4.1.2 3 Task Position and 4 Precision Point Example

A four-bar mechanism is desired to guide a rigid body through the 3 task positions and 4 precision points given in Table 4.3. The equations, as presented in Ch. 2 applied to this problem

27

Figure 4.2: One four-bar linkage that can satisfy the task in Table 4.1.

are,

$$\mathbf{L}_{1j} \cdot \overline{\mathbf{L}}_{1j} - \mathbf{L}_{11} \cdot \overline{\mathbf{L}}_{11} = 0 \qquad \mathbf{L}_{2j} \cdot \overline{\mathbf{L}}_{2j} - \mathbf{L}_{21} \cdot \overline{\mathbf{L}}_{21} = 0, \qquad j = 2, \ldots, 7. \tag{4.3}$$

Since the orientation for precision-points 3, 4, 5 and 6 are variables,

$$\mathbf{T}_j \overline{\mathbf{T}}_j = 1, \qquad j = 3, \ldots, 6. \tag{4.4}$$

This polynomial system of 16 equations in the 16 complex variables may be listed in two groups $\{\mathbf{G}_1, \mathbf{G}_2, \mathbf{z}_1, \mathbf{z}_2, \mathbf{T}_3, \mathbf{T}_4, \mathbf{T}_5, \mathbf{T}_6\}$ and $\{\overline{\mathbf{G}}_1, \overline{\mathbf{G}}_2, \overline{\mathbf{z}}_1, \overline{\mathbf{z}}_2, \overline{\mathbf{T}}_3, \overline{\mathbf{T}}_4, \overline{\mathbf{T}}_5, \overline{\mathbf{T}}_6\}$.

Using Bertini, 252000 paths were tracked and 3116 solutions were identified. After post-processing, 48 real solutions were found corresponding to 24 actual linkages. The solutions for G_{1_x} and G_{1_y} are shown as isolated points in Fig. 4.3.

28

Table 4.2: All solutions for the 4 task position and 2 precision point listed in 4.1

Sol.	G_{1x}	G_{1y}	G_{2x}	G_{2y}
1	26.72	20.54	21.62	13.60
2	24.79	19.63	27.46	11.97
3	26.43	20.44	26.50	5.41
4	26.31	20.40	27.23	11.75
5	21.62	13.71	26.40	20.43
6	24.29	5.65	27.80	12.28
7	34.28	7.42	36.87	19.72
8	-17.73	-35.00	24.25	5.65
9	-17.71	-34.98	27.83	12.31
10	22.80	17.62	32.57	17.99
11	26.48	20.46	-516.60	-543.90

4.1.3   2 Task Position and 6 Precision Point Example

A four-bar mechanism is desired to guide a rigid body through the 2 task positions and 6 precision points as shown in Table 4.4. The equations, as presented in Ch. 2, applied to this problem are,
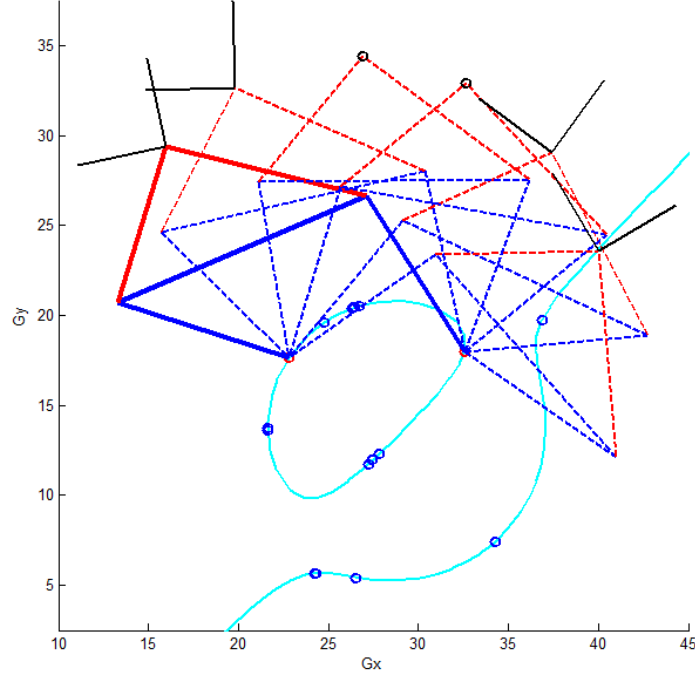
$$\mathbf{L}_{1j} \cdot \overline{\mathbf{L}}_{1j} - \mathbf{L}_{11} \cdot \overline{\mathbf{L}}_{11} = 0 \qquad \mathbf{L}_{2j} \cdot \overline{\mathbf{L}}_{2j} - \mathbf{L}_{21} \cdot \overline{\mathbf{L}}_{21} = 0, \qquad j = 2, \dots, 8. \qquad (4.5)$$

Since the orientation for precision-points 2, 3, 4, 5, 6 and 7 are variables,

$$\mathbf{T}_j \overline{\mathbf{T}}_j = 1, \qquad j = 2, \dots, 7. \qquad (4.6)$$

This polynomial system of 20 equations in the 20 complex variables may be listed in two variable groups $\{\mathbf{G}_1, \mathbf{G}_2, \mathbf{z}_1, \mathbf{z}_2, \mathbf{T}_2, \mathbf{T}_3, \mathbf{T}_4, \mathbf{T}_5, \mathbf{T}_6, \mathbf{T}_7\}$ and $\{\overline{\mathbf{G}}_1, \overline{\mathbf{G}}_2, \overline{\mathbf{z}}_1, \overline{\mathbf{z}}_2, \overline{\mathbf{T}}_2, \overline{\mathbf{T}}_3, \overline{\mathbf{T}}_4, \overline{\mathbf{T}}_5, \overline{\mathbf{T}}_6, \overline{\mathbf{T}}_7\}$.

Bertini was not able to generate the number of paths being tracked. This is not a limitation of Bertini but one of available computational resources.

Table 4.3: Combined task consisting of 3-positions and 4-points

j	d_{j_x}	d_{j_y}	θ_j(deg)
1	14.167	16.093	151.14
2	16.859	30.380	99.08
3	39.508	25.345	38.85
4	13.300	24.164	–
5	23.200	34.090	–
6	28.706	34.231	–
7	34.338	31.924	–

Table 4.4: Combined task consisting of 2 task positions and 6 precision points

j	d_{j_x}	d_{j_y}	θ_j(deg)
1	24.12	11.54	102.07
2	0.45	-9.83	30.45
3	10.45	23.43	–
4	1.22	25.17	–
5	-5.66	24.14	–
6	-10.28	22.23	–
7	-15.46	18.56	–
8	17.98	18.88	–

4.2   Combinations having a One-Parameter Set of Solutions

As discussed in the previous section, numerical solutions can be generated for the combination of tasks with finite solutions. Combinations with a one-parameter set of solutions can be determined by solving the finite problem at multiple orientations for a task position. Consider the case of the the 4 task position, 1 precision point task. The range of solutions can be generated by solving the 5 task position and 0 precision point task for various $0 \leq \theta_5 \leq 2\pi$, as shown in Fig. 4.4. Likewise, the
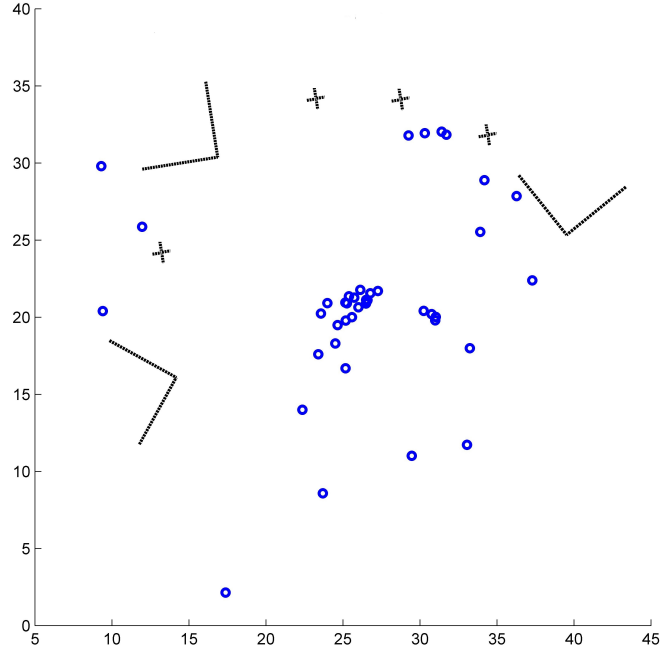
Figure 4.3: G_{1x} and G_{1y} solutions that satisfy the task in Table 4.3.

3 task position and 3 precision point synthesis solution set can be generated from multiple discrete solutions of the 4 task position and 2 precision point case.

4.2.1   4 Task Position and 1 Precision Point Example

A four-bar mechanism is desired to guide a rigid body through the 4 task position and 1 precision point given in Table 4.5. For this 4 task positions and 1 precision point task, the 5 task position and 0 precision point task will be solved for discrete values in the range $0 \leq \theta_3 \leq 2\pi$, as in the example is shown in Fig. 4.4.

Without $\mathbf{T}_3$ and $\overline{\mathbf{T}}_3$ as variables, Eqs. 2.9 and 2.10, $j = 2, \ldots, 5$, become bilinear and readily simplifies the solution. The Bertini software tracked 70 paths. Since the same system of equations
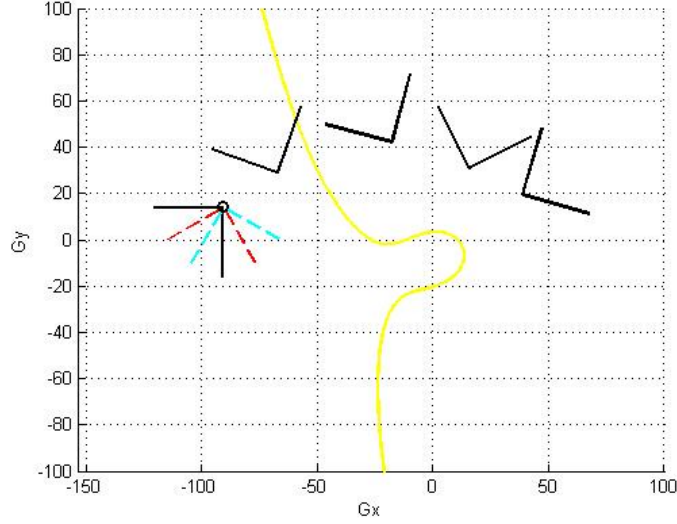
Figure 4.4: 4-position 1-point synthetis

is to be iteratively solved with different values of $\mathbf{T}_3$, a user-defined homotopy was used to further streamline the process. This method allows the user set up the complete computation process with Bertini only for solving the first value of $\mathbf{T}_3$. The solution from solving the first value of $\mathbf{T}_3$ is used as the starting system to be tracked for the following iterative computation. The steps of tracking is significantly reduced, for example, from 70 to 20 compared with the computation of first value of $\mathbf{T}_3$. The center-point curve for the 4 task positions is shown in Fig. 4.4. The $\mathbf{G}_1$ and $\mathbf{G}_2$ solutions to the 4 task position 1 precision point problem are a subset of this curve. Only a subset of the four-bar linkages that satisfy the 4 task positions do not reach the precision point. For the ranges of the center-point curve that do not contain solutions to the 4 task position and 1 precision point problem, the boundary points occur when the RR dyad has reached the edge of its workspace. This means that at one of the task specifications, the proximal and distal links have become parallel as shown in Fig 4.7. In other terms, $\mathbf{L}_{1j}$ is parallel to $\mathbf{T}_j\mathbf{z}_1$, which is ensured by the relation,

$$\mathbf{T}_j\mathbf{z}_1\overline{\mathbf{L}}_{1j} - \overline{\mathbf{T}}_j\overline{\mathbf{z}}_1\mathbf{L}_{1j} = 0. \tag{4.7}$$

Table 4.5: Task combination with 4 task positions and 1 precision point

j	d_{jx}	d_{jy}	θ_j(deg)
1	22.13	11.54	-24.15
2	20.98	22.88	6.93
3	10.45	23.44	–
4	5.23	27.17	54.14
5	-5.66	24.14	78.02

as detailed in Sec. 2.2. Linkages that satisfy the task constraints and are at the edge of the workspace

can be solved by adding Eq. 4.7 to the other synthesis constraints of Eqs. 2.9 and 2.10, $j = 2, \ldots, 5$,

and Eq.2.4, j = 3. Bertini produced 7 real solutions for this example. The solutions for G_{1x} and G_{1y}

are shown as circles in Fig. 4.6 and labeled $\mathbf{G}_A, \ldots, \mathbf{G}_G$. The values for the seven points appear in

Table 4.6.

Table 4.6: The locations for the boundary points for the task given in Table 4.5

G	G_x	G_y
$\mathbf{G}_A$	6.87	5.52
$\mathbf{G}_B$	6.78	4.87
$\mathbf{G}_C$	-5.20	22.96
$\mathbf{G}_D$	7.06	6.03
$\mathbf{G}_E$	6.78	4.84
$\mathbf{G}_F$	1.61	5.59
$\mathbf{G}_G$	2.51	12.91

These 7 boundary points divide the center-point curve into 8 ranges as $(-\infty, \mathbf{G}_A),(\mathbf{G}_A, \mathbf{G}_B),...,$

$(\mathbf{G}_F, \mathbf{G}_G),(\mathbf{G}_G, \infty)$. A single $\mathbf{G}_1$ was selected from the center-point curve within each range. A
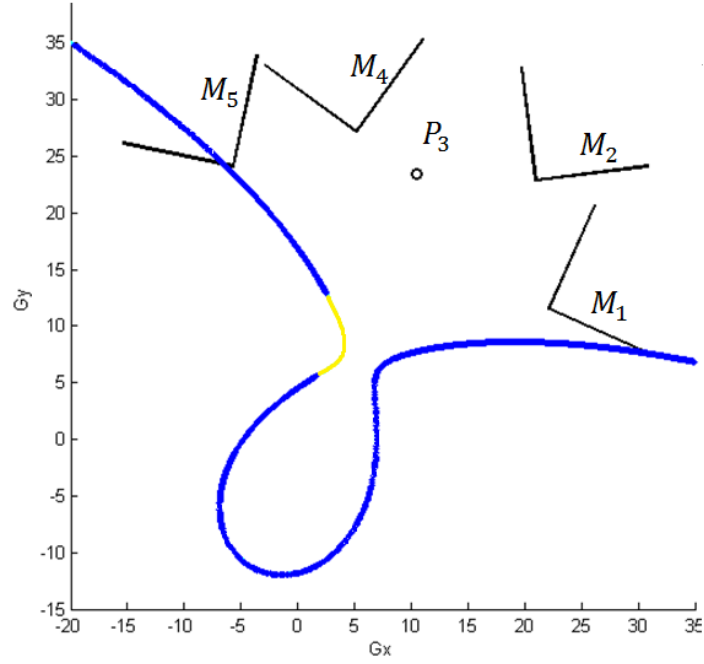
Figure 4.5: G_{1x} and G_{1y} solutions that satisfy the task in Table 4.5

.

dyad was synthesized to achieve the 4 task positions. That dyad was checked as to whether the precision point was within its workspace. In this example, the only dyad that was unable to reach the precision point was in the range of $(\mathbf{G}_B, \mathbf{G}_C)$. Thus, $\mathbf{G}_B$ and $\mathbf{G}_C$ are the boundary points dividing the center-point curve into feasible and unfeasible solutions for the 4 task position and 1 precision point combined synthesis task.

4.2.2 3 Task Position and 3 Precision Point Example

Two examples are introduced in this subsection to show the diversity of solutions that exist for this design challenge. A four-bar mechanism is desired to guide a rigid body through the 3 task position and 3 precision point given in Table 4.7. The numerical solution will be accomplished by solving the 4 task position and 2 precision point problem at discrete values in the range $0 \leq \theta_4 \leq 2\pi$.
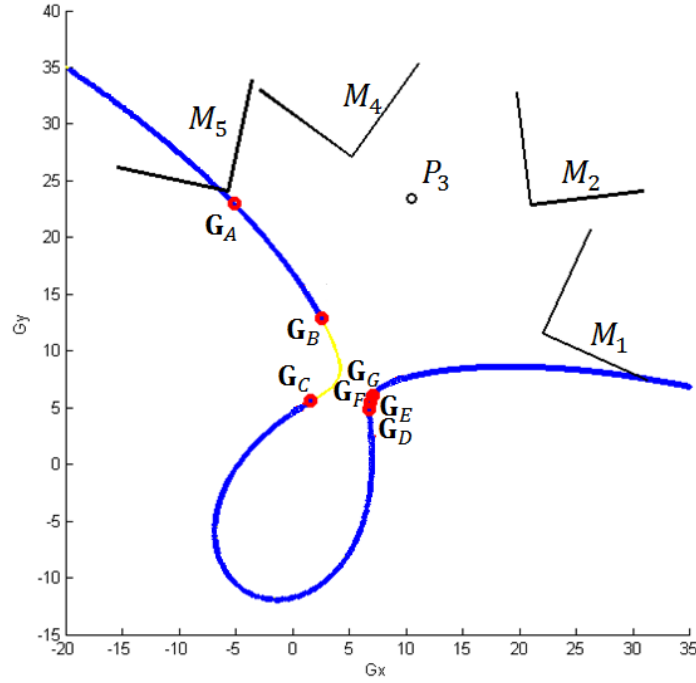
Figure 4.6: Boundary points for the 4-position 1-point solution

The equations, as presented in Ch. 2 and applied to this problem are,

$$\mathbf{L}_{1j} \cdot \overline{\mathbf{L}}_{1j} - \mathbf{L}_{11} \cdot \overline{\mathbf{L}}_{11} = 0 \qquad \mathbf{L}_{2j} \cdot \overline{\mathbf{L}}_{2j} - \mathbf{L}_{21} \cdot \overline{\mathbf{L}}_{21} = 0, \qquad j = 2, \dots, 6. \qquad (4.8)$$

Since the orientation for precision-points 3 and 4 are variables, the

$$\mathbf{T}_j \overline{\mathbf{T}}_j = 1, \qquad j = 3, 4. \qquad (4.9)$$

Thus, the set of 12 polynomial equations mentions those in Sec. 2.1. As before, a user-defined homotopy is used on this iterative process, designating the solution paths to track and streamline the process.

Using a 1° increment for θ_4, the G_{1x} and G_{1y} solutions for each iteration are shown as points in Fig. 4.8. It is observed that this one-parameter set of solutions forms a complicated curve of center points. The choice of any $\mathbf{G}_1$ on Fig. 4.9 is associated with another point $\mathbf{G}_2$, where the dyads are
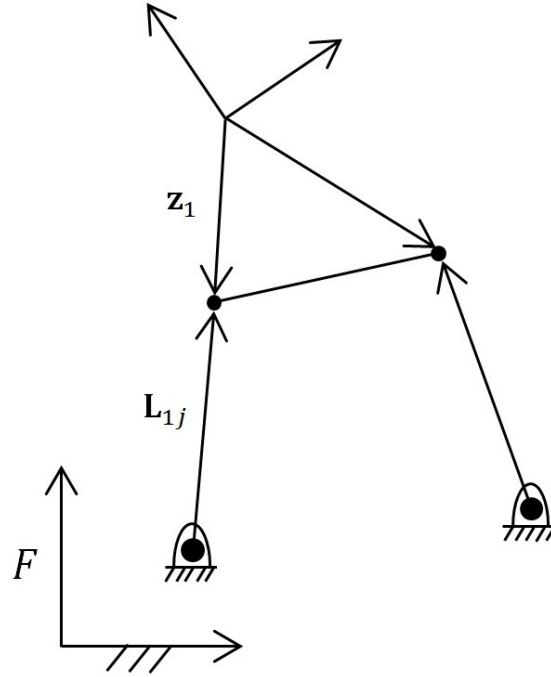
35

Figure 4.7: At a workspace boundary, the proximal and distal links are parallel ($\mathbf{L}_{1j}$ // $\mathbf{T}_j \mathbf{z}_1$) at one specific task position

joined to form a four-bar linkage that can be assembled to satisfy the 3 task positions and 3 precision points task. It is noted that $\mathbf{G}_1$ and $\mathbf{G}_2$ exist in pairs. One of the solutions is shown in Fig. 4.9.

As a second example, a four-bar mechanism is desired to guide a rigid body through the 3 task positions and 3 precision points given in Table 4.8. The set of equations is identical to those in the previous example.

Using a $1°$ increment for θ_4, the G_{1x} and G_{1y} solutions for each iteration are shown as points in Fig. 4.10. It is observed that this one-parameter set of solutions forms a complicated curve of center points. This second example is provided to allow comparison with the other 3 task position and 3 precision point problem in this subsection. Note the considerable differences between the two curves. One of the solutions is shown in Fig. 4.11.

Table 4.7: Task combination with 3 task positions and 3 precision points

j	d_{j_x}	d_{j_y}	θ_j(deg)
1	24.13	11.54	24.15
2	17.98	18.88	36.93
3	10.45	23.44	45.02
4	1.23	25.17	–
5	-5.66	24.14	–
6	-10.28	22.23	–

Table 4.8: Task combination with 3 task positions and 3 precision points

j	d_{j_x}	d_{j_y}	θ_j(deg)
1	-72.67	39.91	72.51
2	-20.22	10.00	15.21
3	57.82	53.08	-63.51
4	5.06	70.00	–
5	-13.32	46.20	–
6	15.22	50.28	–

Figure 4.8: G_{1x} and G_{1y} solutions that satisfy the task in Table 4.7

Figure 4.9: One mechanism solution for the 3 task position and 3 precision point task in Table 4.7
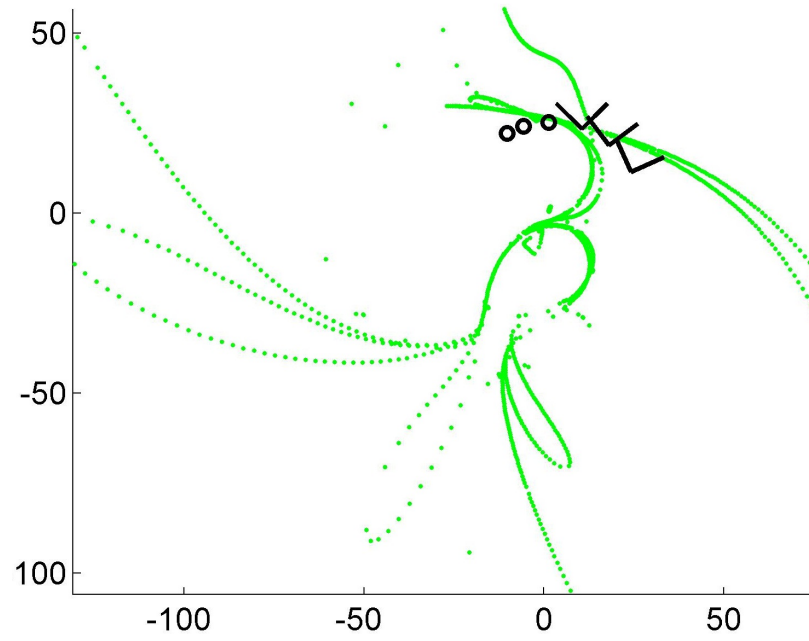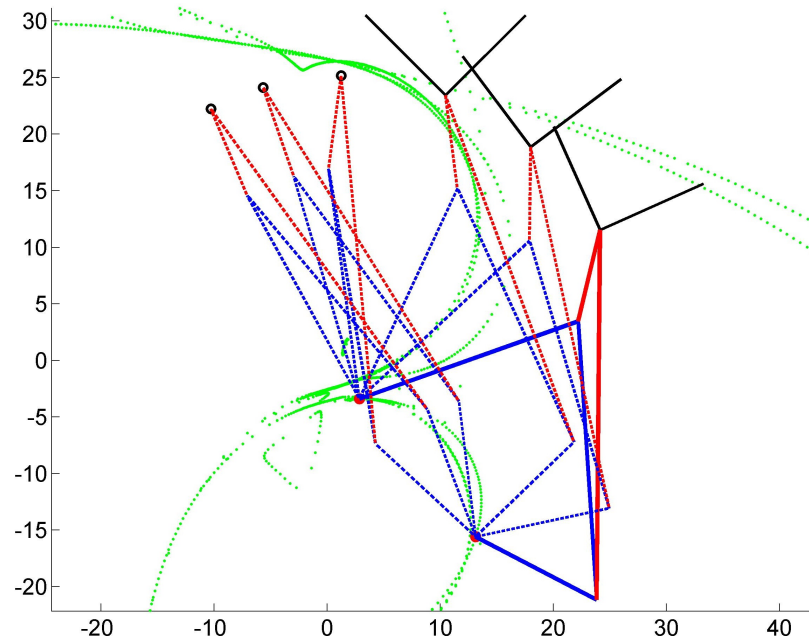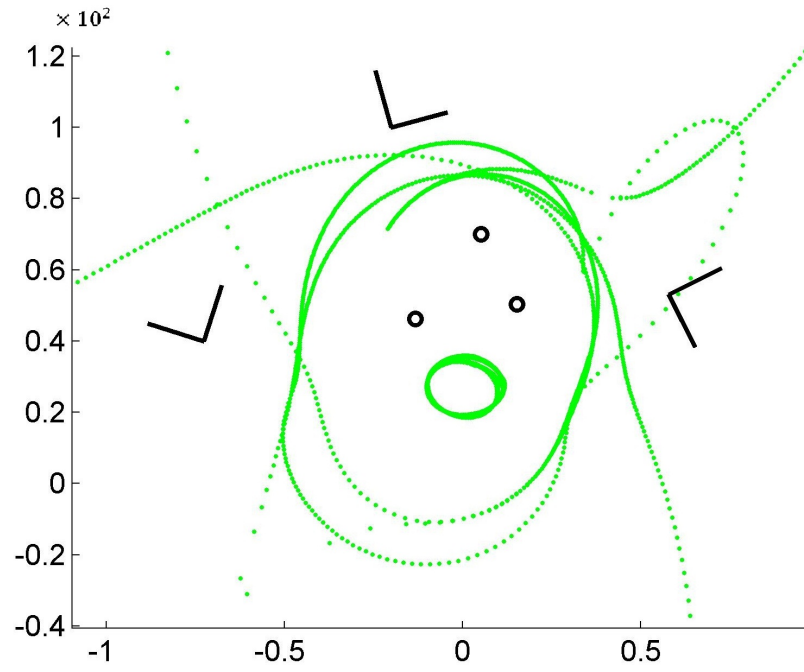
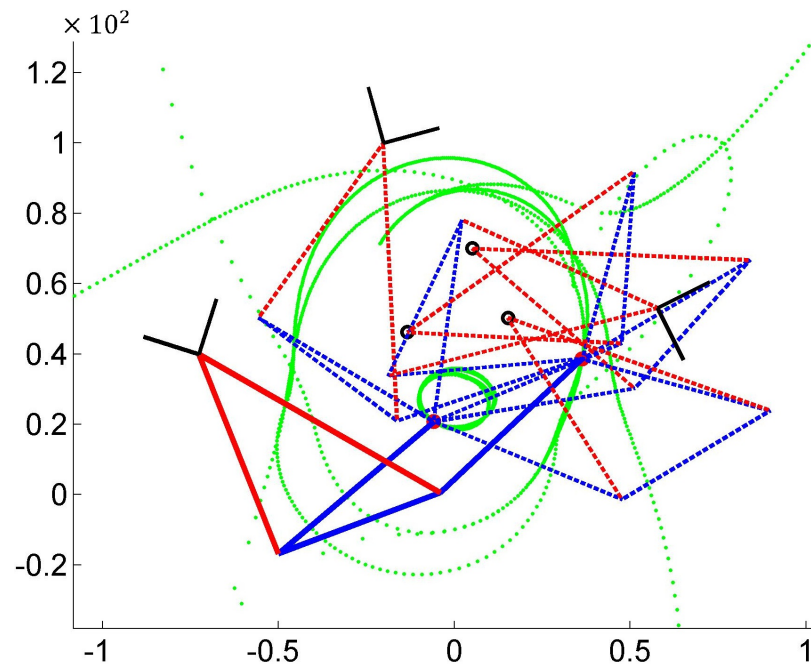Figure 4.10: G_{1x} and G_{1y} solutions that satisfy the task in Table 4.8

Figure 4.11: One mechanism solution for the 3 task position and 3 precision point task in Table 4.8

CHAPTER V

CONCLUSION AND FUTURE WORK

5.1   Conclusion

This thesis developed techniques to design planar four-bar linkages for tasks common to pick-and-place devices. Pick-and-place tasks often require a combination of motion generation and path-point generation. Using isotropic formulations, synthesis equations were formulated and posed as a polynomial system. Counting the synthesis equations and design variables, the combinations of task positions and precision points that have a finite number of four-bar linkages that satisfy the design challenge were presented.

As a first approach, Geometric Constraint Programming (GCP) techniques were used. Location and orientation triangles were constructed and constrained to satisfy the target positions and precision points. After a proposed mechanism was drawn, the triangles could be varied and the linkage was simultaneously regenerated until a desirable linkage was obtained. This method is suitable for the combined synthesis tasks and has the benefit of being intuitive, visual, and expedient (as compared to other techniques). Examples in this work showed GCP techniques as solving 4 task position and 2 precision point, 3 task position and 4 precision point, 2 task position and 6 precision point, 4 task position and 1 precision point and 3 task position and 3 precision point problems.

Numerical techniques were also utilized. Continuation methods were used to solve the polyno-mial system of synthesis equations for tasks that have a finite number of solutions. Iteration methods were also discussed for a combination of tasks that have a single parameter set of solutions. Examples were presented that illustrate linkage synthesis for the 4 task positions and 2 precision points case, 4 task positions and 1 precision point case and the 3 task position and 3 precision point case.

Finally, a methodology was introduced to generate the boundaries of the usable solutions to the 4 task position and 1 precision point case. The methodology relied on identifying those solutions that sat at a singularity of the RR chain.

5.2 Future Work

As introduced in Ch. 3, the solution of discrete points for the combinations of task positions and precision points may be on a specific curve. For example, the solution for 4 task positions and 2 precision points are discrete points on 4 position center point curve. More work is necessary to find the curve for other combinations. Consider the 3 task position and 3 precision point shown in Table 4.8, having the variables $\mathbf{G}_{1_x}, \mathbf{G}_{1_y}, \mathbf{G}_{2_x}, \mathbf{G}_{2_y},$

$\mathbf{z}_{1_x}, \mathbf{z}_{1_y}, \mathbf{z}_{2_x}, \mathbf{z}_{2_y}, \theta_4, \theta_5 \text{ and } \theta_6$. The 10 design equations are,

$$\mathbf{L}_{1j} \cdot \overline{\mathbf{L}}_{1j} - \mathbf{L}_{11} \cdot \overline{\mathbf{L}}_{11} = 0 \qquad \mathbf{L}_{2j} \cdot \overline{\mathbf{L}}_{2j} - \mathbf{L}_{21} \cdot \overline{\mathbf{L}}_{21} = 0, \qquad j = 2, \ldots, 6. \tag{5.1}$$

Define $\mathbf{F}$ as a 10×1 matrix consisting of these 10 equations set. Taking the derivative,

$$\mathbf{M} \cdot \left\{ \begin{array}{c} \partial\,G_{1y} \\ \partial\,G_{2x} \\ \partial\,G_{2y} \\ \partial\,z_{1x} \\ \partial\,z_{1y} \\ \partial\,z_{2x} \\ \partial\,z_{2y} \\ \partial\,\theta_5 \\ \partial\,\theta_6 \end{array} \right\} + \mathbf{V} \cdot \{\partial\,\theta_4\} = \mathbf{0}, \tag{5.2}$$

where $\mathbf{M}$ is the 10×10 Jacobian of $\mathbf{F}$ with respect of variable group without θ_4, and $\mathbf{V}$ is the 10×1 vector of $\mathbf{F}$ derivative with respect of θ_4. That is, the integration of the variables $\mathbf{G}_{1_x}, \mathbf{G}_{1_y}, \mathbf{G}_{2_x}, \mathbf{G}_{2_y}$ may now occur so long as $\mathbf{M}$ is singular establishes bounds in the integration. Finally, solutions to $\mathbf{F}$ at a given value of θ_4 give starting points for an integration that will generate the curve containing all solutions for the 3 task position and 3 precision point example.

BIBLIOGRAPHY

[1] Petlock Incorporated, Juki KE2010L 4-head pick and place surface mount machine, available athttp://www.petlock.com/

[2] Kalpakjian, S., Schmid, S, 2009, *Manufacturing Engineering and Technology*, 6/e, Prentice Hall.

[3] Erdman, A., Sandor, G., Kota, S., 2001, *Mechanism Design: Analysis and Synthesis*, Vol. 1, 4/e, Prentice Hall.

[4] McCarthy, J. M., and Soh, G.S., 2011, *Geometric Design of Linkages*, 2/e, Springer.

[5] Sandor, G., Erdman, A., 1984, *Advanced Mechanism Design: Analysis and Synthesis*, Vol. 2, Prentice Hall.

[6] Burmester, L., 1886, *Lehrbuch der Kinematic*, Verlag Von Arthur Felix, Leipzig, Germany.

[7] Freudenstein, F., Sandor, G., 1959, Synthesis of Path Generating Mechanisms by Means of a Programmed Digital Computer, *ASME Journal for Engineering in Industry*, vol. 81, pp. 2.

[8] Suh, C., Radcliffe, C., 1966, Synthesis of Path Generating Mechanisms with Use of the Displacement Matrix, *Proceedings of the ASME International Design Technical Conferences*, 66-MECH-19, pp. 9.

[9] Morgan, A., Wampler, C., 1990, Solving a Planar Fourbar Design Problem using Continuation, *ASME Journal of Mechanical Design*, vol. 112, No. 4, pp. 544.

[10] Wampler, C., 1992, Complete Solution of the Nine-Point Path Synthesis Problem for Fourbar Linkages, *ASME Journal of Mechanical Design*, vol. 114, No. 1, pp. 153-161.

[11] Mirth, J.A., 1994, The synthesis of planar linkages to satisfy an approximate motion specifications, *Proceedings of the 1993 ASME Design Engineering Technical Conferences*, vol. 53, pp. 65-71.

[12] Diab, N., Smaili, A., 2008, Optimum exact/approximate point synthesis of planar mechanisms, *Mechanism and Machine Theory*, vol. 43, pp. 1610-1624.

[13] Plecnik, M.M. and McCarthy, J.M., 2011, Five Position Synthesis of a Slider-crank Function Generator, *Proceedings of the ASME International Design Technical Conferences*, vol. 6, pp. 317-324.

[14] Mirth, J.A., 1995, Four-Bar Linkages Synthesis for Two Precision Positions Combined With N Quasi-Positions, *ASME Design Engineering Technical Conferences*.

[15] Holte, J.E., Chase, T.T., and Erdman, A.G., 2000, Mixed Exact-Approximate Position Synthesis of Planar Mechanisms, *ASME Journal of Mechanical Design*, vol. 122, pp. 278-286.

[16] Mlinar, J.R. and Erdman, A.G., 2000, An Introduction to Burmester Field Theory, *ASME Journal of Mechanical Design*, vol. 122, pp. 25-30.

[17] Kinzel, E., Schmiedeler, J., Pennock, G., 2006, Kinematic Synthesis for Finitely Separated Positions Using Geometric Constraint Programming, *ASME Journal of Mechanical Design*, vol. 128, No. 5, pp. 1070-1080.

[18] Siemens PLM Software, Solid Edge 2D Drafting, available athttp://www.plm.automation.siemens.com.

[19] Mirth, J.A. and Chase, T.R., 1993, Circuits and Branches of Single-Degree-of-Freedom Planar Linkages, *ASME Journal of Mechanical Design*, vol. 115, No. 2, pp. 223-230.

[20] Mirth, J.A. and Chase, T.R., 1995, Circuit Rectification for Four Precision Position Synthesis of Four-Bar and Watt Six-Bar Linkages, *ASME Journal of Mechanical Design*, vol. 117, No. 4, pp. 612-619.

[21] Balli, S.S., Chand, S., 2002, Defects in Link Mechanisms and Solution Rectification, *Mechanism and Machine Theory*, vol. 37, pp. 851-876.

[22] Heo, J.C., and Yoon, G.H., 2013, Size and configuration syntheses of rigid-link mechanisms with multiple rotary actuators using the constraint force design method, *Mechanism and Machine Theory*, vol. 64, pp. 18-38.

[23] Kramer, G.A., 1992, A Geometric Constraint Engine, *Artificial Intelligence*, vol. 58, pp. 327-360.

[24] Kinzel, E.C., and Pennock, G.R., 2006, Function Generation With Finitely Separated Precision Points Using Geometric Constraint Programming, *Mechanism and Machine Theory*, vol. 64, pp. 1185-1180.

[25] Wampler, C.W., 1999, Solving the Kinematics of Planar Mechanisms *ASME Journal of Mechanical Design*, Vol. 121, 387-391.

[26] Wampler, C.W., 1996, Isotropic Coordinates, Circularity, and Bezout Numbers: Planar Kinematics from a New Perspective, *Proceedings of the ASME Design Technical Conference*, Paper 96-DETC/MECH-1210.

[27] Wampler, C.W., 2001, Solving the Kinematics of Planar Mechanisms by Dixon Determinant and a Complex-Plane Formulation, *ASME J. Mechanical Design*, Vol. 123, pp. 3382–387.

[28] Wampler, C.W., and Sommese, A.J., 2011, Numerical Algebraic Geometry and Algebraic Kinematics, *Acta Numerica*, 469–567.

[29] Bates, D.J., Hauenstein, J.D., Sommese, A.J., and Wampler, C.W., Bertini: Software for Numerical Algebraic Geometry, available at http://www.nd.edu/∼sommese/bertini.

[30] Myszka, D.H., Murray, A.P., and Wampler, C.W. 2012, Mechanism Branches, Turning Curves, and Critical Points, *International Design Engineering Technical Conference*, Paper DETC/MECH-2012.